RSC Advances

PAPER

View Article Online
View Journal | View Issue

Cite this: *RSC Adv.*, 2017, **7**, 9833

A fluorescent chemosensor for Sn^{2+} and Cu^{2+} based on a carbazole-containing diarylethene†

Shengzu Qu, Chunhong Zheng,* Guanming Liao, Congbin Fan, Gang Liu and Shouzhi Pu*

Received 25th November 2016
Accepted 13th January 2017

DOI: 10.1039/c6ra27339d

rsc.li/rsc-advances

A novel diarylethene with a carbazole moiety was developed for the highly selective and sensitive detection of Sn^{2+} and Cu^{2+} in methanol. Its fluorescence was enhanced with a 76 nm blue shift and selective fluorescence quenching occurred upon the addition of Sn^{2+} and Cu^{2+}, respectively, over a wide range of tested cations. The compound formed complexes with Sn^{2+} and Cu^{2+} in a 1 : 1 stoichiometry and has the detection limits of 1.9 μM and 1.2 μM, respectively. Moreover, the compound can be applied to detect Sn^{2+} and Cu^{2+} in natural water samples with high accuracy.

Introduction

Fluorescent sensor design is an active field of supramolecular chemistry due to potential practical advantages in biomedical, analytical, and environmental chemistry,[1] and in the construction of optical and electronic signaling channels towards targeted molecular or ionic species.[2–4] In the last few decades, significant efforts have been made to develop novel fluorescent chemosensors, capable of distinguishing and sensing biologically and environmentally significant cations and anions.[5,6] Among these, the detection of heavy and transition metal ions is significant due to these ions playing crucial roles in living systems and also simultaneously having tremendous detrimental effects when exceeding the normal permissible limits.[7]

Sn^{2+}, an essential trace mineral for humans, is involved in growth factors and cancer prevention.[8] Deficiency of tin may result in poor growth and hearing loss, whereas excess tin accumulation can abhorrently affect respiratory and digestive systems.[9,10] Recent reports have revealed that Sn^{2+} can be readily taken up by human white blood cells and cause DNA damage.[11] Thus, it is of great importance to establish a method for the determination of Sn^{2+} in the environmental and biological systems. Similarly, Cu^{2+} is also of significant importance as it acts as a catalytic cofactor for a variety of metalloenzymes[12] and is an essential trace element for many biological processes and systems.[13,14] The over-accumulation of Cu^{2+} in humans is responsible for many neurodegenerative diseases such as Menkes syndrome,[15,16] Wilson's disease,[17] Alzheimer's disease, and prion disease.[18] Therefore, enormous attempts have been dedicated to the development of Cu^{2+} fluorescent sensors since they facilitate sensitive, easy, and rapid detection.[19]

As one of the most promising photoresponsive materials, diarylethenes have been well-recognized for their remarkable fatigue resistance, excellent thermal stability, and rapid response.[20] Upon alternating the irradiation between UV and visible light, a reversible transformation between the open-ring and closed-ring isomers occurred, accompanied by many obvious changes in the physical properties such as absorption spectra, fluorescence, refractive indices, electronic conduction, oxidation-reduction potentials, and so on. It is very convenient to construct a molecular switch using diarylethenes. Diarylethene derivatives that exhibit good fluorescence performance have become star molecules due to their fluorescence signalling, high detection sensitivity, and simplicity.[21,22] However, most diarylethenes show weak or no fluorescence.[23] Thus, linking a suitable fluorescent chromophore into the diarylethene structure offers new possibilities for developing sensors.[24] To date, many fluorescent sensors for Zn^{2+},[25,26] Cu^{2+},[27,28] Fe^{3+},[29] Al^{3+},[30,31] and Hg^{2+} [32,33] based on diarylethene derivatives have been widely studied. However, there are relatively few reports on the fluorescent sensors for Sn^{2+}.[34,35]

Carbazole possesses a rigid fused-ring structure and its N atom has a lone pair of electrons forming n–π conjugate with benzene rings. It has been widely investigated as a donor due to its potential value for solar energy storage and efficient luminescence.[36] However, the carbazole moiety has rarely been used in diarylethene derivatives.[37,38]

Herein, a novel carbazole-containing diarylethene 1-(2-methyl-5-phenyl-3-thienyl)-2-[2-methyl-5-(3-amine-9-ethyl-carbazolyl)-3-thienyl]perfluorocyclopentene (**1o**) was successfully synthesized. **1o** showed dual channel fluorescence signals ('turn-on' and 'turn-off') for the selective detection of Sn^{2+} and Cu^{2+} in methanol. To the best of our knowledge, this is a new chemosensor for multi-cations (Sn^{2+} and Cu^{2+}) with discrimination in

Jiangxi Key Laboratory of Organic Chemistry, Jiangxi Science and Technology Normal University, Nanchang, Jiangxi 330013, PR China. E-mail: ezirobot@163.com; pushouzhi@tsinghua.org.cn; Fax: +86-791-83831996; Tel: +86-791-83831996

† Electronic supplementary information (ESI) available. See DOI: 10.1039/c6ra27339d

the fluorescence response. Considering the open- and closed-ring isomeric states, the photochromism and ion sensing of the six states was studied to clarify the mechanism of recognition, as shown in Scheme 1.

Experimental

Materials and chemicals

Reactions were monitored by analytical thin-layer chromatography on the plates coated with 0.25 mm silica gel 60 F254 (Qingdao Haiyang Chemical). Flash column chromatography employed silica gel (32–63 μm, Qingdao Haiyang Chemical) and Al_2O_3 (37–74 μm, J&K). Melting points were measured using a WRS-1B melting point apparatus and are uncorrected. Infrared spectra were obtained using a Bruker Vertex-70 spectrometer. NMR spectra were obtained using a Bruker AV-400 spectrometer with teramethylsilane (TMS) as the internal reference and $CDCl_3$ and DMSO-d_6 as solvents. Elemental analysis was carried out using a PE CHN 2400 analyzer. Absorption spectra were obtained using an Agilent 8453 UV/Vis spectrometer. Photoirradiation was carried out using an SHG-200 UV lamp, a CX-21 ultraviolet fluorescence analysis cabinet, and a BMH-250 visible lamp. Light of appropriate wavelengths was isolated by light filters.

Reagents

Chemical reagents were purchased from either Alfa or TCI and used without further purification. Solvents were purchased from Beijing Chemical Works. Anhydrous solvents were of spectro-grade and purified by distillation prior to use. All solution-phase reactions were performed under an atmosphere of dry argon or nitrogen.

Synthesis

The synthesis of **1o** started with the preparation of the intermediates **2** [39] and **3**.[40] **3** was lithiated and coupled with **2** followed by hydrolysis to give **4**, which was further coupled with 9-ethyl-9*H*-carbazol-3-amine to afford **1o**. The synthetic route is shown in Scheme 2.

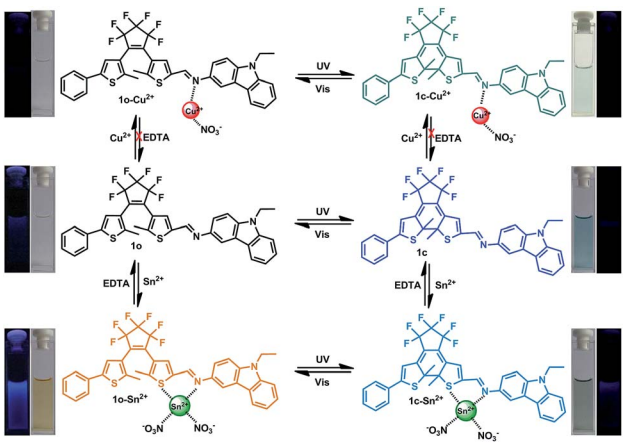

Scheme 1 Photochromism and ion sensing process of **1o**.

Synthesis of 4

To a stirred THF solution (50 mL) of **3** (2.04 g, 10 mmol), 2.5 mol L^{-1} *n*-BuLi/hexane solution (4.40 mL, 11 mmol) was slowly added at 195 K under a nitrogen atmosphere and the mixture was stirred for 30 min. **2** (2.93 g, 8 mmol) was added and the mixture was further stirred for 2 h at this temperature. The reaction was allowed to warm to room temperature and quenched by the addition of water. The product was extracted with diethyl ether and evaporated *in vacuo*. It did not require further purification and was used for the next step reaction. The crude product was dissolved in acetone/water (v/v = 4/1) solution (50 mL) with pyridine (0.79 g, 10 mmol) and *p*-toluenesulfonic acid (2.85 g, 15 mmol). The resulting mixture was refluxed for 6 h and then cooled down to room temperature. The mixture was then sequentially washed with aqueous $NaHCO_3$ and water. After being extracted with ether, the organic layer was dried over $MgSO_4$, filtered, and concentrated. The crude product was purified by column chromatography on silica gel using petroleum ether/ethyl acetate (v/v = 4/1) as the eluent to give **4** (2.12 g) in 45.0% yield. ^{1}H NMR ($CDCl_3$, 400 MHz): δ (ppm) 1.86 (s, 3H, $-CH_3$), 1.98 (s, 3H, $-CH_3$), 7.16 (s, 1H, thiophene-H), 7.30–7.32 (m, 1H, phenyl-H), 7.44–7.46 (m, 2H, phenyl-H), 7.47 (d, 2H, phenyl-H, J = 8.0 Hz), 7.70 (s, 1H, thiophene-H), 9.78 (s, 1H, –CHO); ^{13}C NMR (DMSO-d_6, 100 MHz): δ (ppm) 14.6, 14.7, 123.6, 124.6, 124.8, 125.7, 128.0, 128.4, 129.6, 130.0, 130.6, 133.3, 140.1, 141.5, 183.5.

Synthesis of 1o

4 (0.236 g, 0.5 mmol) and 9-ethyl-9*H*-carbazol-3-amine (0.105 g, 0.5 mmol) were dissolved in methanol (10 mL). The reaction mixture was refluxed for 6 h, and then cooled down to room temperature. The raw product was condensed and purified by recrystallization with methanol to obtain 0.40 g **1o** as a yellow solid in 59% yield. M.p. 378–388 K; ^{1}H NMR (DMSO-d_6, 400 MHz): δ (ppm) 1.38 (t, 3H, $-CH_3$, J = 8.0 Hz), 2.06 (s, 3H, $-CH_3$), 2.08 (s, 3H, $-CH_3$), 4.47–4.54 (m, 2H, $-CH_2$), 7.26 (s, 1H, thiophene-H), 7.40 (s, 1H, thiophene-H), 7.48–7.52 (m, 3H,

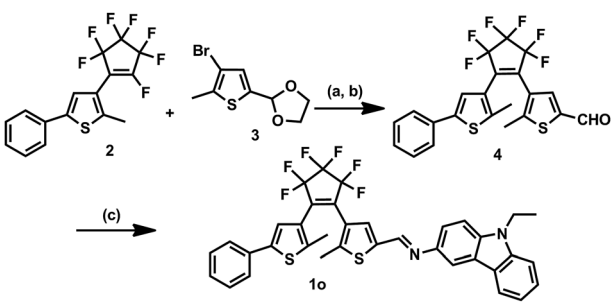

Scheme 2 Synthesis of diarylethene **1o**. Reagents and conditions: (a) *n*-BuLi, THF, 195 K; (b) *p*-TsOH, pyridine, acetone/H_2O, reflux; and (c) 9-ethyl-9*H*-carbazol-3-amine, MeOH, reflux.

benzene-H), 7.56 (d, 2H, J = 8.0 Hz, benzene-H), 7.66–7.72 (m, 4H, benzene-H), 7.77 (s, 1H, benzene-H), 8.24 (d, 2H, J = 8.0 Hz, benzene-H), 9.02 (s, 1H, –CH=N); ^{13}C NMR ($CDCl_3$, 100 MHz): δ (ppm) 13.3, 14.0, 14.5, 37.23, 108.2, 108.3, 112.3, 118.5, 119.4, 120.1, 121.8, 125.2, 125.2, 125.5, 127.5, 128.5, 130.0, 140.1, 148.7; HRMS (ESI$^+$) m/z: 665.1510 $[M + H]^+$, ($C_{36}H_{26}F_6N_2S_2$ requires 664.1442); anal. calcd. for $C_{36}H_{26}F_6N_2S_2$ (%), calcd: C, 70.48; H, 3.91; N, 4.22; found: C, 70.50; H, 3.92; N, 4.21.

Preparation of the metal ions

The solutions of metal ions (0.1 mol L^{-1}) were prepared by the dissolution of their respective metal nitrates in distilled water, except for K^+, Hg^{2+}, Mn^{2+}, and Ba^{2+} (where the counter ion was chloride). Distilled-deionized water was used throughout the experiment.

Procedures for metal-ion sensing

Stock solutions of the metal ions (0.1 mol L^{-1}) were prepared in deionized water. A stock solution of **1o** (1.0×10^{-3} mol L^{-1}) was prepared in CH_3OH, and then diluted to 2.0×10^{-5} mol L^{-1}. Titration experiments were performed by placing 2 mL of **1o** in a quartz cuvette of 1 cm optical path length, and then incrementally adding the Sn^{2+} stock solution by means of a micropipette. Spectra were obtained 3 s after the addition. Test samples for the selectivity experiments were prepared by adding appropriate amounts of metal ion stock solutions to 2 mL of **1o**. In competition experiments, Sn^{2+} or Cu^{2+} was added to the solution containing **1o** and the other metal ions of interest. For fluorescence measurements, excitation was provided at 310 nm, and emission was obtained from 350 to 615 nm.

Determination of cyclization/cycloreversion quantum yields

Quantum yield was measured using 1,2-bis(2-methyl-5-phenyl-3-thienyl)perfluorocyclopentene[41] as reference for the cyclization and cycloreversion reactions. The absorbance of the sample and the reference at the irradiation wavelength (297 nm) were adjusted to be the same for the cyclization quantum yield measurement. The reaction rate of the sample and reference were measured under the same conditions and were compared. For the cyclization quantum yield measurement, absorbance (A) at the absorption maximum of the closed-ring isomer was plotted against time. For the cycloreversion quantum yield measurement, $-\log A$ at the absorption of the irradiated wavelength was plotted against time. The measurement was carried out five times, and the value was determined by averaging.

Determination of the stoichiometry of the 1o–Sn^{2+}/Cu^{2+} complexes

According to the method for continuous variation, a series of solutions of **1o** and Sn^{2+}/Cu^{2+} at ratios of 1 : 9, 2 : 8, 3 : 7, 4 : 6, 5 : 5, 6 : 4, 7 : 3, 8 : 2, and 9 : 1 were prepared, and the fluorescence spectra were obtained. When plotting the fluorescence intensity against $[M^{2+}]/([M^{2+}] + [\mathbf{1o}])$, a feature point was obtained at 0.5 on the abscissa, indicating the 1 : 1 stoichiometry of the **1o**–Sn^{2+}/Cu^{2+} complexes.

Determination of the association constant (K_a)

According to the fluorescence titration, the apparent association constant (K_a) was determined using the following equation: $F - F_0 = \Delta F = [M^{2+}](F_{max} - F_0)/(K_a + [M^{2+}])$, where F is the observed fluorescence, F_{max} is the saturated fluorescence for the **1o**–Sn^{2+} or **1o**–Cu^{2+} complex, and F_0 is the fluorescence for the free **1o**. When plotting the reciprocal of ΔF against the reciprocal of concentration of Sn^{2+} or Cu^{2+}, a linear relation equation was obtained: $Y = A + BX$. K_a was calculated from A/B.

Determination of the limit of detection (LOD)

The detection limit was calculated based on the fluorescence titration. To determine the S/N ratio, the emission intensity of **1o** without any metal ions was measured 15 times and the standard deviation of the blank measurements was determined. Three-independent duplication measurements of emission intensity were performed in the presence of metal ions and each average value of the intensities was plotted as a concentration of metal ions for determining the slope. The detection limit was then calculated using the equation: detection limit = $3\sigma/A$, where σ is the standard deviation of the blank measurements and A is the slope of intensity plotted *versus* sample concentration.

Real sample analysis

The water sample was filtered through a filter paper to remove some large-size impurities. The solutions of Sn^{2+}/Cu^{2+} (0.01 mol L^{-1}) were prepared by the dissolution of $Sn(NO_3)_2$/$Cu(NO_3)_2$ in distilled water (standard solutions) and river water (sample solutions), respectively. The intensity for each of the four standard solutions was determined at 477/401 nm for the fluorescence spectrum. The results were obtained and the working curve was prepared. The intensity of the sample solutions was determined to find out the concentration of Sn^{2+}/Cu^{2+} by the working curve method.

Results and discussion

The photochromic behavior of **1o** was examined in methanol (2.0×10^{-5} mol L^{-1}) at room temperature (Fig. 1A). The absorption maximum of the open-ring form was observed at

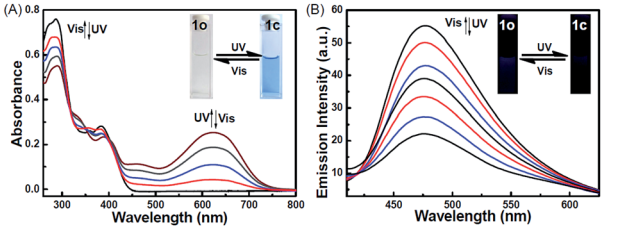

Fig. 1 Absorption spectral and color changes in the absorption and fluorescence of **1o** upon alternating irradiation between UV and visible light in methanol: (A) absorption and color changes (2.0×10^{-5} mol L^{-1}) and (B) fluorescence and color changes (2.0×10^{-5} mol L^{-1}), excited at 310 nm.

287 nm due to the $\pi \rightarrow \pi^*$ transition.[42] Upon irradiation with 297 nm light, the absorption at 287 nm decreased, and a new absorption band centered at 622 nm emerged due to the formation of the closed-ring isomer **1c**, accompanied with a color change from colorless to blue. The blue color could be bleached to colorless upon irradiation with visible light ($\lambda > 500$ nm), and the absorption spectrum returned to the initial state of **1o**. The cyclization and cycloreversion quantum yields were 0.22 and 0.028, respectively. Moreover, the compound showed good stability at room temperature. No decomposition was detected when the powder was exposed to air for more than six months. After 50 repeat cycles (Fig. S1†), the degradation for **1c** was only 7.6%. The fluorescence property of **1o** was measured in methanol (2.0×10^{-5} mol L^{-1}) at room temperature (Fig. 1B). When excited at 310 nm, the fluorescent emission peak of **1o** appeared at 477 nm. Upon irradiation with 297 nm light, the emission intensity decreased due to the formation of weakly fluorescent closed-ring isomers of **1c**.[43] The back-irradiation with appropriate visible light ($\lambda > 500$ nm) regenerated the open-ring isomer of **1o**, and the emission intensity returned to the original state. When the photostationary state was achieved, the emission intensity of **1** was quenched to *ca.* 40%.

The fluorometric responses of **1o** towards metal ions was studied in methanol. The fluorescence of **1o** was not significantly influenced in the presence of metal ions such as Zn^{2+}, Co^{2+}, Mn^{2+}, Hg^{2+}, Pb^{2+}, Cd^{2+}, K^{+}, Ca^{2+}, Mg^{2+}, Ba^{2+}, Sr^{2+}, and Ni^{2+}. However, the emission intensity of **1o** was selectively altered upon the addition of Sn^{2+}/Cu^{2+}. As shown in Fig. 2, a clear fluorescence enhancement of **1o** with a 76 nm blue shift was observed with Sn^{2+}, whereas a reverse response, *i.e.* fluorescence quenching, was observed upon the addition of Cu^{2+}. The enhancement with Sn^{2+} has been explained based on the inhibition of C=N isomerization due to chelate formation.[44]

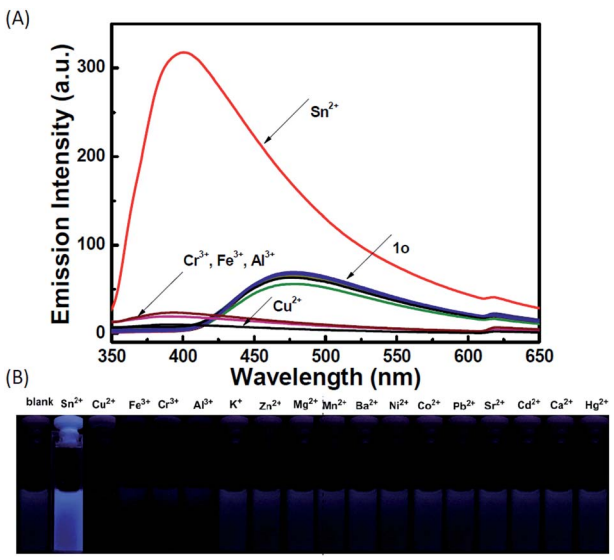

Fig. 2 Changes in the fluorescence of **1o** induced by the addition of various metal ions (12 equiv.) in methanol (2.0×10^{-5} mol L^{-1}): (A) emission spectral changes and (B) images demonstrating changes in the fluorescence.

Moreover, the blue shift indicated that the possible intramolecular charge transfer occurred in **1o** on interaction with Sn^{2+}. In contrast, the fluorescence quenching by Cu^{2+} was most likely due to an energy transfer process occurring from **1o** to the open-shell d-orbitals and paramagnetic Cu^{2+}, which caused a faster and more efficient nonradiative decay of the excited states of **1o**. Moreover, Cr^{3+}, Al^{3+}, and Fe^{3+} exerted a slight quenching effect with a 76 nm blue shift. However, compared with the strong fluorescence quenching by Cu^{2+}, their disturbances were quite minor.

To determine the binding stoichiometry between **1o** and Sn^{2+}/Cu^{2+}, the continuous variation method was used. Fig. 3 displays the Job's plot of the fluorescence intensity of **1o** and the intensity of the system with the molar fraction of the host $\{[\mathbf{1o}]/([\mathbf{1o}] + [Sn^{2+}/Cu^{2+}])\}$ for a series of solutions, in which the total concentration of **1o** and Sn^{2+} or Cu^{2+} was constant with the molar fraction of **1o** continuously varying. The inflection point was observed when the molar fraction reached 0.5, which indicates a 1 : 1 binding stoichiometry between **1o** and Sn^{2+}/Cu^{2+}. The formation of the **1o**–Sn^{2+}/Cu^{2+} complex was confirmed by ESI mass spectra (Fig. S2†). The free **1o** displayed a characteristic peak at 665.1 *m*/*z*. When excess amounts of Sn^{2+} were added to **1o**, a new peak at 907.5 *m*/*z* emerged that was assigned to **1o**–Sn^{2+} (the calculated $[\mathbf{1o} + Sn^{2+} + 2NO_3^{-} - H]$ value was 908.0). When excess amounts of Cu^{2+} were added to **1o**, a new peak at 788.1 *m*/*z* emerged that was assigned to **1o**–Cu^{2+} (the calculated $[\mathbf{1o} + Cu^{2+} + NO_3^{-} - H]^{+}$ value was 789.1). The complex formation was further confirmed by IR (Fig. S3†) and ^{1}H NMR (Fig. S4†) spectra, respectively. In the IR spectra, the 1669 cm^{-1} ν(C=N) peak of **1o** shifted to 1599 cm^{-1} due to the reaction with Sn^{2+} and that of **1o** shifted to 1674 cm^{-1} due to the formation of a bond between –C=N and Cu^{2+}. The new peak at 1380/1388 cm^{-1} indicated that NO_3^{-} was introduced into **1o**–Cu^{2+} and **1o**–Sn^{2+}, respectively.[45] In the ^{1}H NMR spectra of **1o**–Sn^{2+}, the proton (–CH=N) signal at 9.03 ppm showed up-field shifts upon the addition of Sn^{2+}. This indicated that Sn^{2+} binds to the imine moiety. However, the proton signals could not be detected in the presence of the paramagnetic Cu^{2+}. The possible complex formation is shown in Scheme 1.

The fluorescence spectral titrations of **1o** (2.0×10^{-5} mol L^{-1}) were performed with incremental addition of Sn^{2+}/Cu^{2+} to obtain a better idea of the binding constants and binding stoichiometry (Fig. 4). When excited at 310 nm, the fluorescence intensity of **1o** at 477 nm was enhanced more than 4.5-fold with a 76 nm blue shift for Sn^{2+} and quenched more than 5-fold with

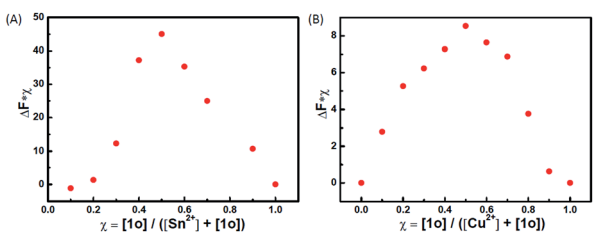

Fig. 3 Job's plot showing the 1 : 1 complex: (A) **1o** with Sn^{2+}, and (B) **1o** with Cu^{2+}.

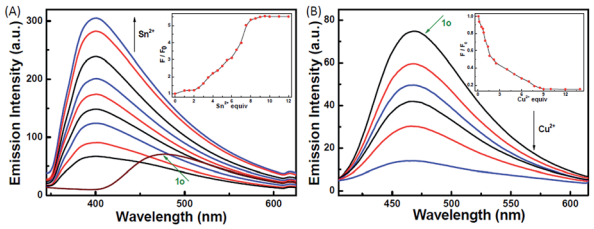

Fig. 4 Changes in the fluorescence of **1o** induced by the successive addition of Sn^{2+} and Cu^{2+} in methanol (2.0×10^{-5} mol L^{-1}): (A) Sn^{2+} and (B) Cu^{2+}. Inset: fluorescence intensity at 477/401 nm for **1o** as a function of the concentration of Sn^{2+} and Cu^{2+}, respectively.

Cu^{2+}. The association constant K_a was graphically evaluated by plotting $F_0/(F - F_0)$ against $1/[M^{2+}]$, as shown in Fig. 5. The fluorescence titration data were linearly fitted according to the Benesi–Hilderbrand equation,[46,47] which indicated 1 : 1 binding stoichiometry. The K_a values were obtained from the slope and intercept of the line and the calculated binding constants were 4.04×10^3 L mol^{-1} and 3.40×10^4 L mol^{-1} for Sn^{2+} and Cu^{2+}, respectively. The standard deviation for the three repeated measurements of K_a was 0.88% for Sn^{2+} and 1.48% for Cu^{2+}. Under optical detection, according to the reported method,[48] the detection limit of **1o** as a fluorescent sensor for Sn^{2+}/Cu^{2+} was determined from the plot of fluorescence intensity as a function of the concentration of Sn^{2+}/Cu^{2+} (Fig. S5†). **1o** was found to have the detection limits of 1.9×10^{-6} and 1.2×10^{-6} mol L^{-1}, respectively, which is reasonable for the detection of micromolar concentrations of Sn^{2+}/Cu^{2+}.

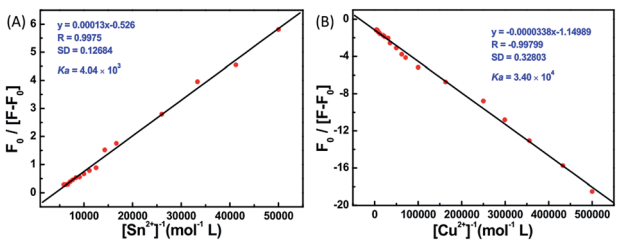

Fig. 5 The Benesi–Hildebrand plots based on the 1 : 1 complexes: (A) **1o**–Sn^{2+} and (B) **1o**–Cu^{2+}.

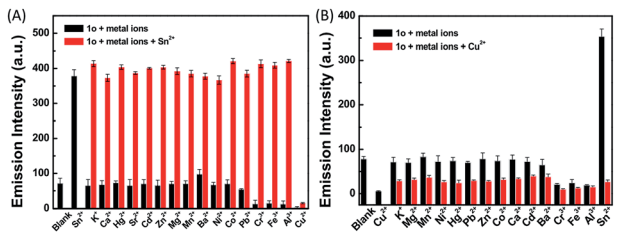

Fig. 6 Emission intensity change upon the addition of different interfering metal ions in methanol (2.0×10^{-5} mol L^{-1}): (A) **1o** + Sn^{2+} and (B) **1o** + Cu^{2+}. Bars represent the emission intensity at 477/401 nm. Black bars represent the addition of 10 equiv. of various metal ions to the solution of **1o** and red bars represent the addition of Sn^{2+}/Cu^{2+} (20 equiv.) to the abovementioned solution.

To check the interference of other metal ions in the detection of Sn^{2+} and Cu^{2+}, the interference studies were carried out by monitoring the change in the emission profile of **1o**–Sn^{2+}/Cu^{2+} in the presence of other interfering cations (Zn^{2+}, Al^{3+}, Cr^{3+}, Co^{2+}, Mn^{2+}, Hg^{2+}, Pb^{2+}, Cd^{2+}, K^+, Ca^{2+}, Fe^{3+}, Mg^{2+}, Ba^{2+}, Sr^{2+}, and Ni^{2+}). As shown in Fig. 6, the fluorescence profile of **1o** with Sn^{2+} was not affected by the coexistence of other interfering metal ions except Cu^{2+}. In the presence of Cu^{2+}, the fluorescence intensity decreased almost 5-fold, which may be ascribed to the high association constant of **1o** for Cu^{2+}. Even in the presence of Sn^{2+}, the fluorescence intensity obviously decreased upon the addition of Cu^{2+}. These studies show that no other metal ions are interfering in the detection of Sn^{2+} except Cu^{2+} and the specific response for Cu^{2+} is not disturbed by other competing metal ions.

To understand the reversibility of **1o** towards Sn^{2+}/Cu^{2+}, a reversibility experiment was carried out using disodium salt of ethylene diamine tetraacetate (Na_2EDTA), which has a strong binding ability towards metal ions. As shown in Fig. 7, upon the addition of 12 equiv. of EDTA to **1o** containing Sn^{2+}, the emission intensity immediately decreased. Further addition of Sn^{2+} could restore the fluorescent state. The cycle (Sn^{2+}–EDTA) can

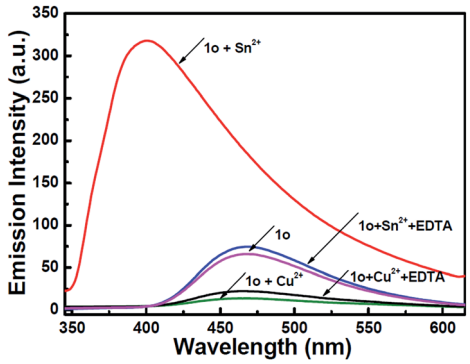

Fig. 7 Reversible binding of **1o**–Sn^{2+}/Cu^{2+} with EDTA. Fluorescence of **1o**, **1o** in the presence of Sn^{2+}/Cu^{2+}, respectively, and (c) probe in the presence of Sn^{2+}/Cu^{2+} upon the addition of excess amount of EDTA.

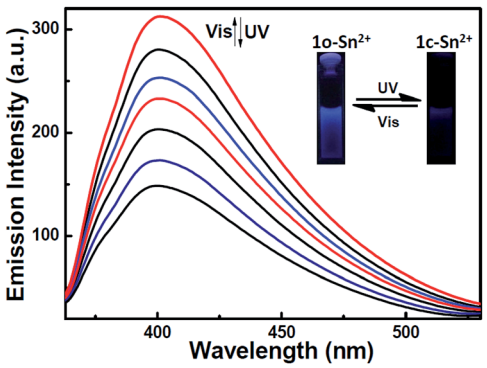

Fig. 8 Fluorescence spectral and color change of **1o**–Sn^{2+} upon alternating irradiation between UV and visible light in methanol (2.0×10^{-5} mol L^{-1}) excited at 310 nm.

Table 1 Detection of Sn^{2+} in natural water samples

Sample	Sn^{2+} added (nM)	Sn^{2+} determined (nM)	Recovery (%)
1	120	127.1	105.9
2	130	141.2	108.6
3	140	151.2	108.0
4	150	166.5	111.0

Table 2 Detection of Cu^{2+} in natural water samples

Sample	Cu^{2+} added (nM)	Cu^{2+} determined (nM)	Recovery (%)
1	40	44.3	111
2	60	58.0	96.6
3	80	73.7	92.2
4	100	94.7	94.7

be carried out four times. This regeneration indicates that **1o** can be reused with proper treatment, whereas the fluorescence could not be regained by further addition of excess EDTA, indicating irreversible sensing for Cu^{2+}.

The effect of pH on the fluorescence intensity of **1o** was investigated in the absence and presence of Sn^{2+}/Cu^{2+}. As shown in Fig. S6,† no obvious fluorescence intensity change of **1o** was observed between pH 2.4 and 11.5, suggesting that the compound is stable over a wide range. In the pH range of 4.0–11.5, a marked fluorescence enhancement was observed upon the addition of Sn^{2+}. In the presence of Cu^{2+}, the quenched fluorescence was almost unaffected over a wide range, from pH 2.4 to 12.9. Therefore, **1o** can detect Sn^{2+} and Cu^{2+} over a wide pH range with a high selectivity and specificity.

Moreover, **1o**–Sn^{2+} exhibited a notable fluorescent switch by photoirradiation, as shown in Fig. 8. The emission intensity of the complex **1o**–Sn^{2+} notably decreased upon irradiation with 297 nm light due to the formation of the closed-ring isomer of **1c**–Sn^{2+}. When arriving at the photostationary state, the emission intensity was quenched *ca.* 52%. The back irradiation with appropriate visible light regenerated the open-ring isomer **1o**–Sn^{2+} and recovered its original emission intensity.

To demonstrate the real application of **1o**, Sn^{2+}/Cu^{2+} in real water samples from the Ganjiang River of Nanchang City were determined according to the reported methods.[49,50] Different amounts of Sn^{2+}/Cu^{2+} were spiked into the real water sample. The sample was filtered through a 0.2 mm membrane. Tables 1 and 2 show the results obtained using the fluorescent sensor **1o** with appropriate added amounts of Sn^{2+}/Cu^{2+}. The recovery for both Sn^{2+} and Cu^{2+} was over 90%. Therefore, **1o**, which can detect Sn^{2+}/Cu^{2+} in real water samples with high accuracy, has practical value.

Conclusions

A novel diarylethene with a carbazole unit, which shows high sensitivity and selectivity for Sn^{2+} and Cu^{2+} in methanol over a wide range of metal ions tested, was designed and synthesized. The sensing of Sn^{2+} and Cu^{2+} was not affected in the presence of other interfering cations. The 1 : 1 stoichiometry complexes were confirmed from Job's plot with the detection limits were 1.9 μM for Sn^{2+} and 1.2 μM for Cu^{2+}. Moreover, the compound showed high accuracy for Sn^{2+} and Cu^{2+} in natural sample testing. The results indicate that diarylethene derivatives can be used for practical applications in sensory research.

Acknowledgements

The authors are grateful for the financial support received from the National Natural Science Foundation of China (21363009, 21362013, 51373072), the Science Funds of Natural Science Foundation of Jiangxi Province (20142BAB203005, 20132BAB203005), the Young Scientist Training Program of the Jiangxi Province (20153BCB23008), and the JXSTNU Sci-Tech innovation team (2015CXTD002), the Project of the Science Funds of Jiangxi Education Office (GJJ160774).

Notes and references

1 T. Q. Duong and J. S. Kim, *Chem. Rev.*, 2010, **110**, 6280–6301.
2 J. M. Lehn, *Supramolecular Chemistry—Conceptand Perspective*, VCH, Weinheim, 1995.
3 M. Chhatwal, A. Kumar, V. Singh, R. D. Gupta and S. K. Awasthi, *Coord. Chem. Rev.*, 2015, **292**, 30–55.
4 G. R. C. Hamilton, S. K. Sahoo, S. Kamila, N. Singh, N. Kaur, B. W. Hyland and J. F. Callan, *Chem. Soc. Rev.*, 2015, **44**, 4115–4132.
5 L. Basabedesmonts, D. N. Reinhoudt, M. Cregocalama, S. Sahoo, J. Marek and N. Singh, *Chem. Informationsdienst*, 2007, **36**, 993–1017.
6 A. Kuwar, R. Patil, A. Singh and Y. T. Yang, *J. Mater. Chem. C*, 2014, **3**, 453–460.
7 M. Vendrell, D. Zhai, J. C. Er and Y. T. Yang, *Chem. Rev.*, 2012, **112**, 4391–4420.
8 H. Rüdel, *Ecotoxicol. Environ. Saf.*, 2003, **56**, 180–189.
9 N. Cardarelli, *Thymus*, 1990, **15**, 223–231.
10 L. R. Sherman, J. Masters, R. Peterson and S. Levine, *J. Anal. Toxicol.*, 1986, **10**, 6–9.
11 C. M. Viau, J. M. Cardone, T. N. Guecheva, M. L. Yoneama, J. F. Dias, F. G. Sousa, C. Pungartnik, M. Brendel and J. A. Henriques, *Arch. Toxicol.*, 2009, **83**, 769–775.
12 B. E. Kim, T. Nevitt and D. J. Thiele, *Nat. Chem. Biol.*, 2008, **4**, 176–185.
13 J. Y. Jung, M. Kang, J. Chun, J. Lee, J. Kim, Y. Kim, S. J. Kim, C. Lee and J. Soon, *Chem. Commun.*, 2013, **49**, 176–178.
14 V. K. Gupta, M. R. Ganjali and P. Nayak, *Anal. Chem.*, 2011, **41**, 282–313.
15 S. Lutsenko, A. Gupta, J. L. Burkhead and V. Zuzel, *Arch. Biochem. Biophys.*, 2008, **476**, 22–32.
16 M. Didonato and B. Sarkar, *Biochim. Biophys. Acta*, 1997, **1360**, 3–16.
17 E. Gaggelli, H. Kozlowski, D. Valensin and G. Valensin, *Chem. Rev.*, 2006, **106**, 1995–2004.

18 H. Kozlowski, M. Luczkowski, M. Remelli and D. Valensin, *Coord. Chem. Rev.*, 2012, **256**, 2129–2141.
19 E. L. Que, D. W. Domaille and C. J. Chang, *Chem. Rev.*, 2008, **108**, 1517–1549.
20 M. Irie, *Chem. Rev.*, 2000, **100**, 1685–1716.
21 X. Q. Chen, T. Pradhan, F. Wang, J. S. Kim and J. Yoon, *Chem. Rev.*, 2012, **112**, 1910–1956.
22 K. P. Carter, A. M. Young and A. E. Palmer, *Chem. Rev.*, 2014, **114**, 4564–4601.
23 M. Irie, T. Fukaminato, K. Matsuda and S. Kobatake, *Chem. Rev.*, 2014, **114**, 12174–12277.
24 S. Z. Pu, Q. Sun, C. B. Fan, R. J. Wang and G. Liu, *J. Mater. Chem. C*, 2016, **4**, 3075–3093.
25 X. J. Piao, Y. Zou, J. C. Wu, C. Y Li and T. Yi, *Org. Lett.*, 2009, **11**, 3818–3821.
26 C. C. Zhang, S. Z. Pu, Z. Y. Sun, C. B. Fan and G. Liu, *J. Phys. Chem. B*, 2015, **119**, 4673–4682.
27 Q. Zou, X. Li, J. J. Zhang, J. Zhou, B. Sun and H. Tian, *Chem. Commun.*, 2012, **48**, 2095–2097.
28 C. H. Zheng, G. Liu, S. Z. Pu and B. Chen, *Tetrahedron Lett.*, 2013, **54**, 5791–5794.
29 S. Y. Huang, Z. Y. Li, S. S. Li, J. Yin and S. H. Liu, *Dyes Pigm.*, 2012, **92**, 961–966.
30 J. Q. Ren and H. Tian, *Sensors*, 2007, **7**, 3166–3178.
31 S. Z. Pu, C. C. Zhang, C. B. Fan and G. Liu, *Dyes Pigm.*, 2016, **129**, 24–33.
32 L. Xu, S. Wang, Y. N. Lv, Y. A. Son and D. Cao, *Spectrochim. Acta, Part A*, 2014, **128**, 567–574.
33 T. Fukaminato, T. Sasaki, T. Kawai and M. Irie, *J. Am. Chem. Soc.*, 2004, **126**, 14843–14849.
34 S. S. Wei, C. H. Zheng, G. Liu, B. Chen and S. Z. Pu, *J. Photochem. Photobiol., A*, 2015, **307–308**, 48–53.
35 S. Z. Pu, Y. M. Xue, C. H. Zheng, W. W. Geng, S. Q. Cui and G. Liu, *Tetrahedron*, 2014, **70**, 9070–9076.
36 Z. R. Grabowski, K. Rotkiewicz and W. Rettig, *Chem. Rev.*, 2003, **103**, 3899–4031.
37 Y. Xing, H. Lin, F. Wang and P. Lu, *Sens. Actuators, B*, 2006, **114**, 28–31.
38 Z. J. Zhao, Y. J. Xing, Z. X. Wang and P. Lu, *Org. Lett.*, 2007, **9**, 547–550.
39 A. Peters, C. Vitols, R. McDonald and N. R. Branda, *Org. Lett.*, 2003, **5**, 1183–1186.
40 S. L. Gilat, S. H. Kawai and J. M. Lehn, *J. Chem. Soc., Chem. Commun.*, 1993, 1439–1442.
41 M. Irie, T. Lifka, A. S. Kobatake and S. Kobatake, *J. Am. Chem. Soc.*, 2000, **122**, 4871–4876.
42 Z. X. Li, L. Y. Liao, W. Sun, C. H. Xu, C. Zhang, C. J. Fang and C. H. Yan, *J. Phys. Chem. C*, 2008, **112**, 5190–5196.
43 T. Kawai, M. S. Kim, T. Sasaki and M. Irie, *Opt. Mater.*, 2003, **21**, 275–278.
44 B. N. Ahamed and P. Ghosh, *Dalton Trans.*, 2011, **40**, 6411–6419.
45 C. W. Frank and L. B. Rogers, *Inorg. Chem.*, 2002, **5**, 1543–1548.
46 H. A. Benesi and J. H. Hildebrand, *J. Am. Chem. Soc.*, 1949, **71**, 2703–2707.
47 M. Barra, C. Bohne and J. C. Scaiano, *J. Am. Chem. Soc.*, 1990, **112**, 8075–8079.
48 D. L. Massart, B. G. Vandeginste, L. M. C. Buydens, S. De Jong, P. J. Lewi and J. S. Verbeke, *Handbook of Chemometrics and Qualimetrics: Part A*, Eselvier, Amsterdan, Netherlands, 1997, ch. 13.
49 Y. T. Chen, Y. S. Mi, Q. F Xie, J. N. Xiang, H. L. Fan, X. B. Luo and S. R. Xia, *Anal. Methods*, 2013, **5**, 4818–4823.
50 X. Wu, J. Chen and J. X. Zhao, *Analyst*, 2013, **138**, 5281–5287.